



<http://www.diva-portal.org>

Postprint

This is the accepted version of a paper presented at *The 15th International Conference on Wireless and Mobile Computing (WiMob 2019) Barcelona, Spain 21-23 october.*

Citation for the original published paper:

Sundberg, S., Garcia, J. (2019)

Localization Performance for eNodeBs using Solitary and Fused RSS-Modeling Approaches

In: *IEEE International Conference on Wireless and Mobile Computing, Networking, and Communications* IEEE

<https://doi.org/10.1109/WiMOB.2019.8923521>

N.B. When citing this work, cite the original published paper.

© 2019 IEEE. Personal use of this material is permitted. Permission from IEEE must be obtained for all other uses, in any current or future media, including reprinting/republishing this material for advertising or promotional purposes, creating new collective works, for resale or redistribution to servers or lists, or reuse of any copyrighted component of this work in other works.

Permanent link to this version:

<http://urn.kb.se/resolve?urn=urn:nbn:se:kau:diva-75899>

# Localization Performance for eNodeBs using Solitary and Fused RSS-Modeling Approaches

Simon Sundberg

Dept. of Mathematics and Computer Science  
Karlstad University, Sweden  
Email: simon.sundberg@kau.se

Johan Garcia

Dept. of Mathematics and Computer Science  
Karlstad University, Sweden  
Email: johan.garcia@kau.se

**Abstract**—The problem of locating radio devices has been addressed by a variety of methods. In the cellular setting, most of the focus has been on locating user equipment (UE). This work focuses on the inverse problem, i.e. locating the eNodeB based on received signal strength (RSS) measurements collected by UEs. We perform a comprehensive evaluation of six variations of two RSS-modeling based localization approaches. Furthermore, two methods for fusing the location estimates of the individual cells were also examined. The evaluation is done using a manually created ground truth data set for eNodeB positions, and a large measurement data set comprising of more than four million observations collected from cellular modems onboard Swedish trains. The best localization accuracy was obtained by one of our proposed variations of logloss fitting using geographic aggregation with highest mean RSRP as the reference point selection criteria. When combined with centroid-based fusion of the individual cell estimates, a median eNodeB localization error of 433 m was obtained, which is a considerable improvement over the second-best approach which achieved a median error of 674 m. The centroid-based fusion approach was found to consistently outperform the DPD fusion approach, which in turn had a better localization error distribution than obtained for solitary cells.

## I. INTRODUCTION

Knowing the position of LTE base stations can be beneficial in a number of circumstances. For example, a train may be equipped with a system to provide internet access to passengers. If such a system includes directional external antennas, knowledge of base station positions may be useful to tune antenna parameters. The position of cellular infrastructure can also be useful information in the context of cognitive radio, as well as when verifying operator provided coverage maps. Unfortunately, the position of cellular infrastructure is commonly not publicly available as operators generally do not wish to share this data for business or security reasons.

There are several different approaches to wireless localization. However, many of them require specialized equipment such as antenna arrays to detect the angle of incoming signals for Angle of Arrival (AoA) methods, or precise time measurements and synchronization required by Time of Arrival (ToA) and Time Difference of Arrival (TDoA) methods. When such information is not

available, a solution is to use Received Signal Strength (RSS) methods as they only require measurements of signal strength, which most radio devices can provide. Most work on the application of RSS methods in cellular networks focuses on locating the mobile terminal from the network side, for example to comply with FCC demands for locating devices calling 911 [1] or to enable location based services. In this work we however consider the reverse case, locating network infrastructure, more specifically LTE base stations, through measurements from user equipment (UE). In particular, we consider the case where measurements were collected by cellular modems on board trains traveling along the railway track. Using an evaluation data set of more than four million data points, we evaluate several variants of the RSS-modeling based location estimation methods. We consider the case of base stations which are transmitting on several sectors as well as on multiple frequencies, and also evaluate two different methods for fusing the location estimations from individual cells into one eNodeB location estimate. The results show that one of our proposed variants, coupled with centroid-based fusion, provides the best eNodeB localization performance with a median error of 433 meters. The second best approach had a median error of 674 meters.

The paper is structured as follows. The next section discusses related work, followed by an overview of the RSS-modeling based localization approaches to be evaluated. Section IV discusses the two fusion approaches employed while Section V describes the evaluation setup. Section VI presents the results, followed by the conclusions.

## II. RELATED WORK

Localization of transmitters with an unknown transmission power is a challenge which can be solved with the Power Difference of Arrival (PDoA) method. In [2] an FM radio station is located using PDoA, and [3] uses the PDoA method with a swarm of Unmanned Aerial Vehicles (UAVs) to locate radio frequency emitters. In [4], several different versions of PDoA methods are evaluated through both simulations and real measurements. Other

methods based on modeling the RSS through propagation losses have also been proposed, such as the Monte Carlo Path Loss Simulation method used to locate indoor WiFi access points in [5], and the method used in [6] to locate a Very High Frequency (VHF) transmitter in an urban area.

Some previous attempts to locate cellular infrastructure using UE measurements have used crowd-sourced data, but the use of such data may be hampered by differences between the devices used to collect the measurements. In [7] several simple methods, such as using the centroid of all measurements or the center of the minimal enclosing circle, were evaluated for locating GSM base stations using a crowd-sourced data set collected through smartphone clients. Overall, a grid-based approach is found to perform the best. A similar recent study is [8], which also evaluates several different methods on a crowd-sourced data set. No single method is found to consistently outperform the others, and a supervised machine learning approach, called Adaptive Algorithm Selection is proposed to select the method that is most likely to provide the best result for a specific cell. A supervised machine learning approach is also utilized in [9], which employs a Multi Layer Perceptron neural network to directly locate GSM base stations through measurements collected with a smartphone app in a small urban area of Istanbul.

### III. RSS-MODELING BASED LOCALIZATION

The network of primary interest here, LTE, has an access network (also known as Evolved Universal Terrestrial Radio Access Network (E-UTRAN)) essentially consisting of a single type of node, the Evolved NodeB (eNodeB), which is interconnected with other eNodeBs and the core network. Each eNodeB may have several different antennas, covering different sectors or using different carrier frequencies, each of them known as a cell. Each cell is identifiable through its E-UTRAN Cell Identifier (ECI), which contains an eNodeB identifier that is unique within the Public Land Mobile Network (PLMN) [10]. In the following subsections, the general principle of propagation modeling is described along with the specific metrics used, followed by a presentation of the evaluated position estimation methods.

#### A. Propagation modeling

The basic principle behind RSS based localization methods is to use measurements of RSS to estimate the distance to the receiver from multiple points, in order to derive the position of the transmitter. To estimate the distance based on RSS, a propagation model is used. A common model which is both flexible and simple is the log distance path loss model, described by (1).

$$P_r = P_0 - 10\alpha \log \frac{d}{d_0} + X_\sigma \quad (1)$$

Here  $\alpha$  is the path loss exponent,  $P_r$  is the received power at distance  $d$  from the transmitter and  $P_0$  is the received power at some known reference distance  $d_0$  from the transmitter. The random variable  $X_\sigma$  is used to model various shadowing effects, and has through measurements been shown to be a 0-mean normal distribution with some standard deviation  $\sigma$  in the decibel scale (a so called log-normal distribution) [11].

In LTE, there are primarily two metrics that are used to measure the RSS, Received Signal Strength Indicator (RSSI) and Reference Signal Received Power (RSRP). The 3GPP defines RSSI as the linear average of the total power from all resource elements for specified OFDM symbols over some number  $N$  resource blocks, including noise and interference [12]. On the other hand, RSRP is defined as the linear average of the power contributions from resource elements that carry cell-specific reference signals over some measured bandwidth.

While the 3GPP does not specify any scheme for downlink power control in LTE, it does demand that the transmit power for the cell-specific reference signals used for determining RSRP should remain constant until a new transmit power is signaled. Hence, any active power control the operator may chose to use in downlink should have a limited impact on RSRP. In addition, RSRP should not be systematically affected by the measured bandwidth and does not include noise and interference, and therefore RSRP was chosen over RSSI as the metric to use for the RSS methods in this study.

In this work, multiple variants of two different RSS based localization methods that work for transmitters with unknown transmission power are used. The first method is based on logloss fitting and has previously been considered in a Monte Carlo Path-loss Fitting Simulation context [5]. The second method is based on a Power Difference of Arrival (PDoA) algorithm. As the cells of an eNodeB may use different carrier frequencies and transmission power, as well as covering areas with different radio environments, the methods have been applied on the data for each cell individually instead of using them to directly locate the eNodeBs. To combine the results from multiple cells to create a joint estimate for the eNodeB location, two merging schemes have been used, which are further explained in Section IV.

#### B. Logloss-based transmitter position estimation

The logloss fitting method is based on finding the position for the transmitter which results in observations having the best possible fit to the log distance path-loss model shown in (1). Assuming that the transmitter is at some candidate location  $x, y$ , a log distance path-loss model can be fitted to all  $I$  RSS measurements by solving the linear least squares problem:

$$\operatorname{argmin}_{P_0, \alpha} \sum_{i=1}^I \left( P_{r_i} - \left( P_0 - 10\alpha \log \frac{d_i}{d_0} \right) \right)^2 \quad (2)$$

$$d_i = \sqrt{(x - x_i)^2 + (y - y_i)^2}$$

However, whereas [5] used ordinary least squares, we instead use a version of the Trust Region Reflective algorithm from [13] (as implemented by scipy [14]) to allow bounds to be set on  $P_0$  and  $\alpha$ . Setting up bounds prevents a good fit from being obtained by using unreasonable values for  $P_0$  or  $\alpha$ , for example by using a negative path loss exponent.  $P_0$  was limited to values between -140 and 0 dBm at a reference distance of 100 m, and  $\alpha$  was allowed to vary between 1 and 8. The transmitter coordinates  $\hat{x}, \hat{y}$  are then found by creating a two-dimensional search grid and fitting the parameters  $P_0$  and  $\alpha$  at each of the  $J$  positions in the grid by solving (2). For each position  $j$ , a cost  $c_j$  is calculated by taking the difference between the measurements and the fitted model as shown in (3), where  $\hat{P}_{r_i}$  is calculated as in (1) with the fitted parameters  $P_0$  and  $\alpha$ . The position with the lowest cost in the search-grid is then selected as the estimated position of the transmitter.

$$c_j = \sum_{i=1}^I \left| P_{r_i} - \hat{P}_{r_i} \right| \quad (3)$$

Two further variations of this method have also been devised, where only  $\alpha$  is fitted with linear least squares and the reference point is chosen by other means. Two different ways of choosing the reference point have been explored, both of which are based on a geographic aggregation scheme to avoid some of the random shadowing effects. The aggregation scheme, which essentially creates a radiomap, divides all measurements into a grid-net, and the center of each grid-cell is given the mean value of all RSRP measurements in the grid-cell. A reference point can then be chosen from the aggregated data by either selecting the grid-cell with the highest mean RSRP, alt1, or the highest number of measurements, alt2.

Figure 1 shows an example of the logloss fitting, as well as the two alternative versions of it, here using the distance from the known position of the eNodeB. The costs for the ordinary logloss fitting method over the entire search-grid for the same cell is shown in Figure 2, with the geographic aggregation of the measurements overlaid on top.

### C. PDoA-based transmitter position estimation

There are several versions of PDoA methods, the one considered here is the Non-Linear Least Squares (NLLS) PDoA algorithm. This version of PDoA was chosen due to results from [4] indicating it had better positioning performance than other versions when the observation

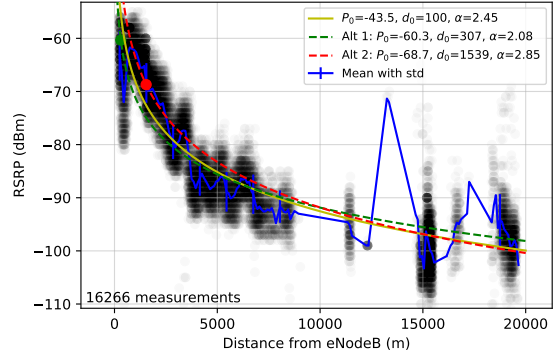


Figure 1. Relationship between distance and RSRP

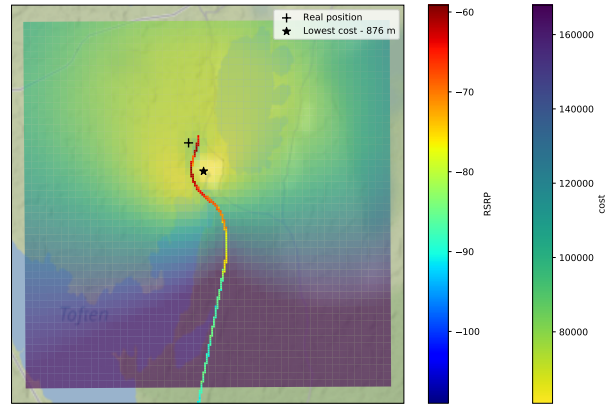


Figure 2. The costs from a logloss fitting search grid over a 10x10 km area using 200x200 m candidate location squares. Also shown are the RSRP values measured along the train track, geographically aggregated into 50x50 m grid cells.

points do not surround the transmitter, which can be expected to be the case here.

Based on the log distance path loss model in (1), the difference in power between two points  $k$  and  $l$  can be estimated as:

$$\hat{P}_{kl} = \hat{P}_k - \hat{P}_l = 10\alpha \log \frac{d_l}{d_k} = 5\alpha \log \left( \frac{(x - x_l)^2 + (y - y_l)^2}{(x - x_k)^2 + (y - y_k)^2} \right) \quad (4)$$

where  $x, y$  is the coordinates of the transmitter. The transmitter is then located by finding the coordinates  $\hat{x}, \hat{y}$  that results in the smallest squared error between the real measured power difference between two points,  $P_{kl}$ , and the estimated power difference  $\hat{P}_{kl}$  from (4), for all  $\frac{I(I-1)}{2}$  pairs of points. This is accomplished by defining a two-dimensional search grid and calculating the deviation from the measurements assuming the transmitter is located at each point in the search grid. In case the path loss exponent  $\alpha$  is unknown, as it is here, this has to be

expanded into a 3-dimensional search grid where  $\alpha$  is varied, in this case between 1 and 8. The NLLS PDoA algorithm is thus equivalent to finding the solution to (5).

$$\operatorname{argmin}_{x,y,\alpha} \sum_{k,l} \left( P_{kl} - 5\alpha \log \left( \frac{(x-x_l)^2 + (y-y_l)^2}{(x-x_k)^2 + (y-y_k)^2} \right) \right)^2 \quad (5)$$

As the number of pairs of points increases with the number of points squared, this method quickly becomes very computationally intensive when a large amount of measurements are used. To make this method feasible even with upwards of 100,000 measurement points, two techniques have been used, random sampling (PDoA samp.) and geographic aggregation (PDoA GA). The geographic aggregation uses the same aggregation scheme used to select reference points for the alternative versions of the logloss fitting method from Section III-B, and uses the grid-cells as input rather than all individual measurements.

#### IV. FUSING MULTIPLE POSITION ESTIMATES

As different cells of an eNodeB may use different transmission power, different carrier frequencies and cover areas with different radio environments, measurements from different cells of an eNodeB cannot be directly compared as required by the logloss fitting and PDoA methods described in Section III-B and III-C. Consequently, the methods have been applied for each cell separately. This results in multiple cost matrices for every eNodeB, where each cost matrix can be used to make an estimate of the eNodeB position. As the transmitters of all cells belonging to an eNodeB should be located at essentially the same location, that of the eNodeB, creating a single joint estimate for the position of the eNodeB is desirable.

The first fusion approach entails using the centroid of all cell estimates for a given eNodeB. This approach thus calculates the average position of the coordinates with the lowest cost in the cost matrix from each cell that belongs to the eNodeB.

The second considered approach represents a more sophisticated way to merge the cost matrices, and is based on the Discrete Probability Density (DPD) method from [15]. The DPD method essentially consists of two steps, converting the cost matrix  $c_i$  for each cell  $i$  into a new matrix  $p_i$  with the properties of a 2D discrete probability mass function (PMF), and then merging the PMF-like matrices for all  $I$  cells of an eNodeB into a single PMF-like matrix  $p$ .

For  $p_i$  to have the properties of a PMF, a higher value of  $p_i(x, y)$  should correspond to an increased likelihood that the eNodeB is located at coordinates  $x, y$ , and  $\sum_x \sum_y p_i(x, y) = 1$ . To convert the  $n \times m$  cost matrix  $c_i$  into  $p_i$ , the costs have first been rescaled into an intermediate matrix  $a_i$  so that all positions sum to 1.

$$a_i(x, y) = \frac{c_i(x, y)}{\sum_x \sum_y^m c_i(x, y)}$$

As a position with higher cost should correspond to a lower probability that the eNodeB is located at that position, all values in  $a_i$  are then inverted and normalized again:

$$p_i(x, y) = \frac{1 - a_i(x, y)}{\sum_x \sum_y^m (1 - a_i(x, y))}$$

Once each cost matrix  $c_i$  has been converted into a corresponding matrix  $p_i$ , they can be merged into a joint PMF-like matrix  $p$  as shown in (6).

$$p(x, y) = \frac{1}{C} \prod_{i=1}^I p_i(x, y) \quad (6)$$

for  $x = 1, \dots, n, y = 1, \dots, m$ , and where  $C$  is used to normalize  $p$  to 1,  $C = \sum_x \sum_y^m \prod_{i=1}^I p_i(x, y)$ . The eNodeB is finally estimated to be at the position with the highest value in  $p$ .

#### V. EVALUATION SETUP

The data set used to evaluate the localization performance for eNodeBs has been collected from the operational logs of a system providing Internet access to passengers onboard trains operating in Sweden. Train passengers are connected to WiFi-access points inside the train carriages which forward the traffic to an aggregation router that aggregates and distributes the traffic on multiple links connected to the cellular network through rooftop antennas. Every five seconds, the system logs data consisting of for example the position, velocity and bearing of the train, as well as individual link throughput, signal-strength and quality measurements for each of the links. Data from the same source has previously been analyzed for different purposes in [16], [17]. This study focuses on a subset of this data consisting of LTE data collected by a single modem type. By using a single modem type, any systematic variations due to differences in hardware implementation are avoided.

To evaluate the accuracy of the location estimates provided by the different methods, the real positions of the eNodeBs have to be established. This information could not be obtained from the operators for this evaluation, so the ground truth was instead manually created. The ground truth was constructed using the user verified cell tower positions from CellMapper<sup>1</sup> as an initial starting point. A coarse-level validation of the location information was then performed by cross-checking the locations with data from OpenCellID<sup>2</sup>, Mozilla Location Service<sup>3</sup> and Google Geolocation API<sup>4</sup>. The final step

<sup>1</sup><https://www.cellmapper.net>

<sup>2</sup><https://www.opencellid.org>

<sup>3</sup><https://location.services.mozilla.com>

<sup>4</sup><https://developers.google.com/maps/documentation/geolocation/intro>

in ground truth creation consisted of visually locating the eNodeBs and manually retrieving their coordinates using Google Maps. In this way ground truth was established for 26 located eNodeBs, which were selected to have measurements from three sectors and with at least two different carrier frequencies. In total 4.3 million measurements were utilized, distributed across 196 cells (belonging to the eNodeBs), and collected by modems on 54 trains over a nine month period between 2018-01 to 2018-10.

The two versions of PDoA described in Section III-C as well as the three versions of logloss fitting described in Section III-B together with Monte Carlo Path Loss Simulation where no bounds on  $P_0$  and  $\alpha$  are set were evaluated for all 196 cells. All methods used the same search grids, and all cells of an eNodeB used a common search grid for that eNodeB. The search grids used a resolution of 200 by 200 meters between the positions, and covered a total of 10 by 10 km centered at the centroid of all measurements of the eNodeB. The size and resolution of the search grid is a compromise between positioning accuracy and computational cost, and the used configuration results in 2500 candidate positions to evaluate in each search grid. For the sampled PDoA method, up to 500 samples from each cell were used, and for geographic aggregation a 50 by 50 meter grid was used.

## VI. POSITIONING ACCURACY EVALUATION

The results from all methods both without any merging, as well as merged with the centroid and DPD schemes, are shown in Table I. The percentage of estimates within 500, 1000 and 2000 m respectively, as well as the median and mean distance between the estimated position and the real eNodeB location, are included. Note that without any merging, the results reflect the distance error distribution for the 196 individual cells, whereas the results for the merged estimates (centroid and DPD) reflect the distance error distribution for the 26 eNodeBs that the cells belong to.

Table I shows that logloss fitting does appear to be an overall improvement over Monte Carlo Path Loss Simulation for the considered data set. Especially the first alternative version of logloss fitting, where the aggregated point with the highest mean RSRP is used as a reference point appears to perform well compared to the other methods, whereas the second alternative version instead performs worse than ordinary logloss fitting. Both of the PDoA methods appear to perform similarly to each other, although overall the sampling approach provides slightly more accurate estimations.

Regarding the merging methods, it is clear that merging the estimates results in an improvement over the individual estimates, and the straightforward centroid merging scheme appears to outperform the DPD method in this case. It is worth noting that the DPD method appears

Table I  
SUMMARIZED RESULTS. PERCENTAGE OF ESTIMATES WITHIN 500, 1000 AND 2000 METERS FROM THE TRUE LOCATION TOGETHER WITH MEDIAN AND MEAN POSITIONING ERROR IN M.

Merge	<500	<1000	<2000	Median	Mean
-------	------	-------	-------	--------	------

### Monte-Carlo Path-loss Fitting Simulation [15]

None	12.76	37.76	61.73	1423	2313
Centroid	15.38	46.15	84.62	1055	1392
DPD	15.38	46.15	73.08	1117	1672

### Logloss fitting

None	18.88	48.47	79.08	1033	1503
Centroid	38.46	65.38	92.31	747	910
DPD	15.38	57.69	88.46	938	1323

### Logloss fitting, alt1

None	22.96	53.06	77.55	892	1615
Centroid	53.85	73.08	92.31	433	890
DPD	19.23	57.69	88.46	886	1291

### Logloss fitting, alt2

None	16.84	43.88	72.45	1151	1728
Centroid	34.62	53.85	92.31	850	1077
DPD	19.23	50.00	88.46	996	1322

### PDOA sampling

None	18.88	48.47	75.00	1035	1659
Centroid	38.46	65.38	92.31	674	1029
DPD	26.92	38.46	76.92	1163	1461

### PDOA Geographic Aggregation

None	17.86	47.45	72.96	1028	1769
Centroid	38.46	61.54	96.15	791	1063
DPD	19.23	38.46	80.77	1178	1464

to work better for the logloss fitting methods than for PDoA, as all columns generally show slightly improved results for DPD compared with no merging for logloss fitting and Monte Carlo Path Loss Simulation, whereas DPD shows worse performance regarding percentage of estimations within 1 km and a higher median distance error for PDoA compared to the individual cell estimates. Of the evaluated methods, the first alternative version of logloss fitting combined with the centroid merging overall produces more accurate position estimates than any other combination.

The current evaluation has focused on approaches that employ RSS-modeling, i.e. uses RSS measurements together with propagation modeling. It can be noted that a number of simple alternate approaches exists.

Computing the centroid of all measurement positions, or additionally weighting the measurement positions with the RSS before computing the centroid are examples of straightforward approaches that have been proposed. Another method is to estimate the eNodeB to be located at the measurement position with the highest RSS. While such relatively simple methods may produce good results in various circumstances, they may also be sensitive to the limited geographical spread of the measurements which are likely to result when the train is linearly following the tracks rather than providing a geographically dispersed set of measurements.

## VII. CONCLUSIONS

This work reports on a comprehensive evaluation of six variations of two RSS-modeling based eNodeB localization approaches. Two methods for fusing the localization estimates of the individual cells were also evaluated. To perform the evaluation, a large evaluation data set of more than four million measurements collected from cellular modems onboard Swedish trains were used, together with a set of 26 eNodeBs with manually established ground truth locations. The best localization accuracy was obtained by one of our proposed variations of logloss fitting using geographic aggregation with highest mean RSRP as reference point selection criteria. When combined with centroid-based fusion of the individual cell estimates, a median eNodeB localization error of 433 m was obtained, which is a considerable improvement over the second-best result from PDoA sampling which achieved a median error of 674 m. The centroid-based fusion approach was found to consistently outperform the DPD fusion approach, which in turn had a better localization error distribution than obtained for solitary cells, although a few exceptions can be found for a couple of individual metrics.

## ACKNOWLEDGMENTS

The authors wish to thank Mats Karlsson, Rikard Reinshagen and Peter Eklund at Icomera AB for the collection of data and discussions on localization methods, and Tobias Vehkajärvi for assistance in processing the data. Funding for this study was provided by the HITS project grant from the Swedish Knowledge Foundation.

## REFERENCES

- [1] FCC, "Wireless E911 Location Accuracy Requirements," Federal Communications Commission, Tech. Rep. 07-114, 2015.
- [2] A. Navarro, W. Cruz, and Y. Castano, "Emitter Location Using Power Difference of Arrival," in *IEEE AP-SURSI 2018*, Jul. 2018.
- [3] S. A. Engebråten, "RF Emitter geolocation using PDOA algorithms and UAVs," Ph.D. dissertation, NTNU - Trondheim, 2015.
- [4] B. R. Jackson, S. Wang, and R. Inkol, "Emitter geolocation estimation using power difference of arrival," *Defence R&D Canada Technical Report DRDC Ottawa TR*, vol. 40, 2011.
- [5] M. Ji, J. Kim, Y. Cho, Y. Lee, and S. Park, "A novel Wi-Fi AP localization method using Monte Carlo path-loss model fitting simulation," in *IEEE PIMRC 2013*, 8.
- [6] A. D. Spirin and B. M. Antipin, "Non-conventional algorithm of radio transmission sources position location," in *IEEE EICoNus 2017*, 1-3 February 2017.
- [7] E. Neidhardt, A. Uzun, U. Bareth, and A. Küpper, "Estimating locations and coverage areas of mobile network cells based on crowdsourced data," in *WMNC 2013*, Apr. 2013, pp. 1–8.
- [8] M.-R. Fida and M. K. Marina, "Uncovering Mobile Infrastructure in Developing Countries with Crowdsourced Measurements," in *ICTD '19*. ACM, 2019.
- [9] A. S. Ogrenci and T. Arsan, "Transmitter source location estimation using crowd data," *Computers & Electrical Engineering*, vol. 66, pp. 127–138, Feb. 2018.
- [10] 3GPP, "Universal Mobile Telecommunications System (UMTS); Numbering, addressing and identification," 3rd Generation Partnership Project (3GPP), Technical Specification (TS) 23.003, Oct. 2018, version 15.5.0 Release 15.
- [11] T. S. Rappaport, *Wireless Communications : Principles and Practice*, 2nd ed. Prentice Hall PTR, 2002.
- [12] 3GPP, "Evolved Universal Terrestrial Radio Access (E-UTRA); Physical layer; Measurements," 3rd Generation Partnership Project (3GPP), Technical Specification (TS) 36.214, Jul. 2018, version 15.2.0 Release 15.
- [13] M. Branch, T. Coleman, and Y. Li, "A Subspace, Interior, and Conjugate Gradient Method for Large-Scale Bound-Constrained Minimization Problems," *SIAM J. Sci. Comput.*, vol. 21, no. 1, pp. 1–23, Jan. 1999.
- [14] E. Jones, T. Oliphant, P. Peterson *et al.*, "SciPy: Open source scientific tools for Python," 2001–. [Online]. Available: <http://www.scipy.org/>
- [15] D. Elsaesser, "The Discrete Probability Density Method for Emitter Geolocation," in *2006 Canadian Conference on Electrical and Computer Engineering*, May 2006, pp. 25–30.
- [16] J. Garcia, S. Alfredsson, A. Brunstrom, and C. Beckman, "Train Velocity and Data Throughput - A Large Scale LTE Cellular Measurements Study," in *2017 IEEE 86th Vehicular Technology Conference (VTC-Fall)*, Sep. 2017.
- [17] J. Garcia, S. Sundberg, A. Brunstrom, and C. Beckman, "Interactions between train velocity and cellular link throughput - an extensive study," in *2019 IEEE International Symposium on Personal, Indoor and Mobile Radio Communications (PIMRC)*, Sep. 2019.